

1 Predicting Hosts Based on Early SARS-CoV-2 Samples and 2 Analyzing Later World-wide Pandemic in 2020

3 Qian Guo^{1#}, Mo Li^{1#}, Chunhui Wang^{1#}, Jinyuan Guo^{1#}, Xiaoqing Jiang^{1#}, Jie Tan¹,
4 Shufang Wu¹, Peihong Wang¹, Tingting Xiao², Man Zhou¹, Zhencheng Fang¹,
5 Yonghong Xiao^{2*} & Huaiqiu Zhu^{1*}

6 ¹ *State Key Laboratory for Turbulence and Complex Systems, Department of
7 Biomedical Engineering, College of Engineering, and Center for Quantitative
8 Biology, and School of life Sciences, Peking University, Beijing 100871, China.*

9 ² *State Key Laboratory for Diagnosis and Treatment of Infectious Diseases, National
10 Clinical Research Center for Infectious Diseases, Collaborative Innovation Center for
11 Diagnosis and Treatment of Infectious Diseases, The First Affiliated Hospital, College
12 of Medicine, Zhejiang University, Hangzhou 310006, China.*

13 [#] These authors contributed equally.

14 * Corresponding authors: hqzhu@pku.edu.cn (Zhu H) & xiao-yonghong@163.com
15 (Xiao Y)

16

17 **Running title:** *Guo Q et al / A host prediction algorithm, DeepHoF*

18

19 **Abstract**

20 The SARS-CoV-2 pandemic has raised the concern for identifying hosts of the virus
21 since the early-stage outbreak. To address this problem, we proposed a deep learning
22 method, DeepHoF, based on extracting the viral genomic features automatically, to
23 predict host likelihood scores on five host types, including plant, germ, invertebrate,
24 non-human vertebrate and human, for novel viruses. DeepHoF made up for the lack of
25 an accurate tool applicable to any novel virus and overcame the limitation of the
26 sequence similarity-based methods, reaching a satisfactory AUC of 0.987 on the five-
27 classification. Additionally, to fill the gap in the efficient inference of host species for
28 SARS-CoV-2 using existed tools, we conducted a deep analysis on the host likelihood

29 profile calculated by DeepHoF. Using the isolates sequenced in the earliest stage of
30 COVID-19, we inferred minks, bats, dogs and cats were potential hosts of SARS-CoV-
31 2, while minks might be one of the most noteworthy hosts. Several genes of SARS-
32 CoV-2 demonstrated their significance in determining the host range. Furthermore, the
33 large-scale genome analysis, based on DeepHoF's computation for the later world-wide
34 pandemic in 2020, disclosed the uniformity of host range among SARS-CoV-2 samples
35 and the strong association of SARS-CoV-2 between humans and minks.

36 **KEYWORDS:** Host prediction; Deep learning, Mink; SARS-CoV-2; Early stage of
37 pandemic

38

39 **Introduction**

40 The global COVID-19 pandemic caused by severe acute respiratory syndrome
41 coronavirus 2 (SARS-CoV-2) has raised the long-lasting quest for hosts of the virus
42 since the pandemic outbreak, meanwhile the majority view is that the virus probably
43 originated from bats [1]. So far there have been many discussions for the potential hosts
44 despite an initial pointer to *Manis javanica* (pangolins) [2, 3], most of the suppositions
45 were based on the increasing cases of animal infection, such as dogs, cats, tigers, lions,
46 and minks [4, 5], *etc.* Several studies performed experiments to investigate the
47 susceptibility of a limited number of model animals [6-8]. At the same time, some
48 studies attempted to reveal the range of hosts based on analysis of molecular sequence
49 or structural information [9, 10]. For instance, Damas *et al.*, [10] conducted a
50 computational analysis based on host receptor similarity using the angiotensin-
51 converting enzyme 2 (ACE2) protein and evaluated the infection risks for a broad range
52 of animals. As the pandemic spreads, minks, which were even not referred to as high
53 infection animal in above peer-review articles, have been frequently reported massively
54 infected with COVID-19 over the world [5], and were the only known animal reported
55 to transmit SARS-CoV-2 to humans [11, 12]. It is worth mentioning that, in January,
56 2020, we have reported in the form of a preprint archive with predicting minks as a
57 potential host based on the six earliest sequenced SARS-CoV-2 isolates [13]. However,

58 the later complication of pandemic prompts peoples again to have a full review of the
59 issue of host determination for SARS-CoV-2. This raises a new challenge, which is how
60 to implement and improve the capability of computational methods to predict the hosts
61 of a novel virus like SARS-CoV-2, especially when we have relatively small amounts
62 of samples of sequencing viral data at the early stage of the pandemic outbreak. It is
63 certainly constructive for similar pandemic caused by novel viruses in the future.

64 Generally, the host range of viruses is dependent on molecular interactions between
65 viruses and host cells including receptor recognition, adaptions to the host cellular
66 machinery and evading innate immune recognition [14]. Of these, receptor recognition
67 that facilitates the attachment of viruses to the host cells is the most primary step. Thus,
68 the glycoproteins that viruses use to recognize the host receptor as well as the whole
69 genome sequences are widely used in identifying the potential hosts of viruses [1]. To
70 detect the potential host and pathogenicity of novel viruses, the conventional
71 computational methods are almost based on similarity of either virus genome
72 composition or host receptor. Limitations of the both strategies lie in that they assume
73 phylogeny may reflect host association. However, this assumption is untenable from
74 the perspective of epidemiology and evolution. On the one hand, viruses occasionally
75 shift between distantly related host species. On the other hand, owing to the long-term
76 adaptation to the hosts, the viral genomic characteristics acquired from hosts can be
77 quite incompatible with the virus phylogenetic groups [15]. The specificity of
78 recognition between viruses and host species also involves structural information in
79 some key domains of both viral proteins and host receptor proteins, such as the receptor-
80 binding domain, that sequence similarity is insufficient to explain. For example, the
81 civet-specific K479 and S487 residues of SARS-CoV spike glycoprotein can efficiently
82 bind to civet ACE2 but have much less affinity to human ACE2 [16, 17]. This is also
83 the reason that the similarity-based method of host ACE2 proteins sequences fails to
84 predict minks as host of high and very high risk for SARS-CoV-2 infection [10].

85 Until now, several published tools aimed to identify the hosts of viruses exceeded
86 the limitation of sequence-similarity-based strategies by machine learning methods

87 with viral sequences or their genomic traits related to virus-host interactions, such as
88 ViralHostPredictor [15], HostPhinder [18], WIsh [19], Host Taxon Predictor [20], and
89 VIDHOP [21]. While these tools performed well under some conditions, they are
90 actually not considered feasible to be applied to a novel virus without the knowledge
91 of host range, like SARS-CoV-2. HostPhinder and WIsh predict hosts for only
92 bacteriophages and they are inappropriate for non-phage viruses. Host Taxon Predictor
93 focuses on distinguish bacteriophages and eukaryotic viruses. ViralHostPredictor
94 predicts hosts and the existence and identity of arthropod vectors for human-infecting
95 RNA viruses by Gradient boosting machines with the features of selected evolutionary
96 genomic traits and phylogenetic information. It also illustrated the better ability of
97 machine learning methods to predict virus hosts compared to the way of sequence
98 similarity comparison. However, ViralHostPredictor cannot determine whether human
99 is the host of a novel virus. With the utilization of evolutionary signatures,
100 ViralHostPredictor lacks power to predict incidental hosts which do not maintain long-
101 term circulation of new viruses. Moreover, the predictive abilities of the methods above
102 rely on the handcrafted features like codon pair scores, *k*-mer frequencies and amino
103 acid biases, which might neglect other important information encoded in the virus
104 genomes. VIDHOP, a deep-learning-based tool, is designed to predict potential hosts of
105 viruses, but its application was limited into three viral species: influenza A, rabies
106 lyssavirus and rotavirus A.

107 To address the challenge of predicting probable hosts of a novel virus like SARS-
108 CoV-2, we proposed the host prediction algorithm DeepHoF (**Deep** learning-based
109 **Host** Finder) in the current study. Developed based on BiPath Convolutional Neural
110 Network (BiPathCNN), DeepHoF automatically extracts the genomic features from the
111 input viral sequences. The model finally outputs five host likelihood scores and their *p*-
112 values on five host types, including plant, germ, invertebrate, non-human vertebrate
113 (refers to other vertebrates except humans) and human, where all the living organism
114 hosts are covered. DeepHoF was designed as a five-class classifier containing five
115 independent nodes in the output layer with sigmoid activation and binary cross-entropy

116 loss function for each node, corresponding to five independent binary classifications on
117 the five host types individually. DeepHoF made up for the lack of efficient method
118 applicable for any novel virus and significantly outperformed the Basic Local
119 Alignment Search Tool (BLAST)-based strategy with the evidently high AUC of 0.987
120 on the classification of five host types. In January 2020, we have reported the host
121 prediction for six earliest sequenced SARS-CoV-2 isolates employing our algorithm
122 [13]. In this study, we furthered the work using the 17 earliest sampled SARS-CoV-2
123 isolates, which provides essential information in the early epidemic of the virus.
124 DeepHoF evaluated the host likelihood scores on humans and non-human vertebrates
125 for the earliest samples and characterized the isolates with their host likelihood score
126 profiles. As there existed a blank in the inference of host species for SARS-CoV-2 using
127 the tools which were state of the art, we conducted a deep analysis on the host likelihood
128 score profile predicted by DeepHoF to find the detailed hosts, including both reservoirs
129 and susceptible hosts which are not discriminated in this study. We inferred minks, bats,
130 dogs and cats were the probable hosts, while minks maybe one of the most noteworthy
131 hosts. The inference was supported by the infection facts or animal experiments in the
132 later pandemic. Based on our model, several genes of SARS-CoV-2 were further
133 investigated and demonstrated their significance in determining the host likelihood
134 scores on human or the host range for SARS-CoV-2, respectively. With a large-scale
135 genome analysis based on DeepHoF's computation for the later world-wide pandemic,
136 the uniformity of host inference among a large number of SARS-CoV-2 samples was
137 verified, and the association of SARS-CoV-2 between humans and minks was disclosed.
138 Supported by the satisfactory performance on five host type classification and the
139 successful application in SARS-CoV-2, DeepHoF has the capability to provide reliable
140 host information of novel virus, and is expected to narrow the time lag between novel
141 virus discovery and prevention at the early-stage of epidemic prevention.

142

143 **Results**

144 **Performance of the DeepHoF algorithm**

145 The DeepHoF algorithm is designed as a five-class classifier using the deep learning
146 method of BiPathCNN (see Methods). Herein five likelihood scores on five host types,
147 including plants, germs, invertebrates, non-human vertebrates, and humans, are
148 calculated by DeepHoF. The host likelihood score profile consisting of five predicted
149 scores, is then analysed in depth to find the specific hosts of a novel virus such as SARS-
150 CoV-2 in this study. As mentioned above, the existed bioinformatics tools [15, 18-21]
151 were not designed to perform the prediction of the host likelihood scores on the five
152 host types for any given virus, and thus cannot be compared with DeepHoF directly.
153 And therefore, we compared the performance of DeepHoF model with BLAST (details
154 of finding host using BLAST are described in Supplementary Methods), adopting six
155 classification metrics: true-positive rate (TPR), false-positive rate (FPR), area under the
156 curve (AUC), precision, accuracy and F1-score. To assess the performance of predicting
157 novel viruses, we used training and test datasets divided in chronological order [22]
158 (Methods). There is no overlap of virus species in training and test sets. With an evident
159 higher AUC of 0.987, DeepHoF can significantly outperform BLAST (with the average
160 AUC of 0.833) as shown in **Figure 1A** and **Table 1** (a detailed comparison on each host
161 type is illustrated in Supplemental Figure S1 and Table S1).

162 In addition, we compared the utility of DeepHoF and a phylogenetic tree to
163 discriminate the human-infecting and non-human-infecting coronaviruses using their
164 whole genome sequences. As shown in Figure 1B (the left), DeepHoF could identify
165 evidently higher probabilities of human-infecting coronaviruses to infect humans (two-
166 sided unpaired Welch Two Sample *t*-test, *p*-value = 1.732×10^{-10}). However, the
167 phylogenetic analysis result was not satisfactory owing to the weak homology among
168 the human-infecting coronaviruses, which were scattered around the phylogenetic tree
169 of coronaviruses (Figure 1C). The comparison was similar for the inferences using their
170 spike glycoprotein coding genes (S genes) as shown in Figure 1B (the right), and D
171 (two-sided unpaired Welch Two Sample *t*-test, *p*-value = 3.657×10^{-5}). This result is
172 nontrivial because S genes are essential in coronavirus-host interaction [23]. Clearly,

173 DeepHoF can overcome the limitation of sequence similarity-based method and shows
174 superior predictive ability especially for novel viruses.

175 **Host prediction of SARS-CoV-2**

176 The accurate prediction of hosts of earliest detected isolates can undoubtedly assist the
177 public health system to take more appropriate preventive measures at the early stage of
178 the pandemic outbreak. In view of this, we focused on the prediction with SARS-CoV-
179 2 isolates sequenced in the earliest stage of COVID-19 detection, which is closer to the
180 most recent common ancestor of SARS-CoV-2. Previous to this paper, we have reported
181 the prediction for the six earliest sequenced SARS-CoV-2 isolates using our algorithm
182 on 21 January, 2020 [13]. In this study, we further strengthened the prediction of hosts
183 of SARS-CoV-2 with all 17 earliest detected isolates (including the six earliest ones)
184 sequenced in December, 2019. Herein we take NC_045512 (complete genome of
185 SARS-CoV-2 isolate, Wuhan-Hu-1, collected on 31 December 2019 in Wuhan, China,
186 and used as the representative genome of SARS-CoV-2 in most studies) as an example
187 to illustrate the workflow of DeepHoF on SARS-CoV-2 isolates (**Figure 2**).

188 For all the 17 SARS-CoV-2 isolates listed in **Figure 3A**, the host likelihood scores
189 on non-human vertebrates and humans were assigned *p*-values less than 0.05 (0.002
190 and 0.027 respectively), illustrating a high possibility of non-human vertebrates and
191 humans (Methods) to be the hosts of SARS-CoV-2. Besides, compared to other
192 coronaviruses released on RefSeq [24], the high similarity of human and non-human
193 vertebrate host likelihood scores among SARS-CoV-2, SARS-CoV and MERS-CoV
194 (Figure 3B), would raise an alarm when the infection capabilities of SARS-CoV-2 was
195 uncertain in the early stage of pandemic.

196 To describe the contribution of each gene in the determination of the host likelihood
197 scores of SARS-CoV-2 isolates (use NC_045512 as a representation), we used each
198 gene sequence of SARS-CoV-2 as the input of DeepHoF and predicted the host
199 likelihood scores for each gene. We found that the S gene, ORF1ab and ORF7b indeed
200 acquired high likelihood scores on human host type and thus playing important roles in
201 determining human as the host (Figure 3C). The fact that several domains on S gene

202 and ORF1ab are essential for the coronavirus-host fusion process, host survival or viral
203 replication [25-27] suggests the rationality of our findings. It is noteworthy that the
204 linear correlation between the lengths and the host likelihood scores for genes is not
205 tenable (Supplemental Figure S2). This shows that the importance of ORF1ab is not
206 due to the remarkable length of the gene. Additionally, our prediction proposes the
207 necessity of further experimental research on the function of ORF7b in SARS-CoV-2.
208 Furthermore, we explored how each gene functioning on coronavirus life circle [25-28]
209 contributed to the human host likelihood scores of SARS-CoV-2, SAR-CoV and
210 MERS-CoV using the earliest sequenced samples, including 12 SARS-CoV isolates, 9
211 MERS-CoV isolates and 17 SARS-CoV-2 isolates released in NCBI in 2003, 2012 and
212 2019, respectively (Supplemental Table S2). The contributions of these genes were
213 represented by their host likelihood scores on human. We found that ORF1ab was
214 relatively important in the prediction for all these viruses, which was possibly due to its
215 functions in viral replication and host survival [27]. The structural genes (S, M, N, and
216 E genes) in these three viruses contributed differently on the human host type,
217 illustrating these genes functioned inconsistently in these viruses. Specifically, S gene,
218 participating in virus-host fusion process, contributed more in SARS-CoV-2 and SARS-
219 CoV, while N gene, eliciting the strong specific antibody responses, played the most
220 important role in MERS-CoV. Two equivalent genes, ORF9b, attaching membrane in
221 virion assembly of SARS-CoV, and ORF8b, related to or immune evasion of MERS-
222 CoV, made high contributions on human host likelihood scores for the two viruses.
223 Moreover, two group-specific genes, ORF7b with unclear function in SARS-CoV, and
224 ORF3 associated with virial replication and pathogenesis in MERS-CoV contributed
225 significantly in the two viruses (Figure 3C, Supplemental Figure S3). These
226 discrepancies might indicate the different significance of these genes among the three
227 coronaviruses in the interaction with human and give hints to the target of drug design.
228 It is disappointed that host determination for SARS-CoV-2 is extremely difficult due to
229 the limited knowledge of the virus world. Therefore, the sequences and host
230 information of viruses contained in the public database should be valued and fully

231 utilized. To fill the gap in the efficient inference of host species for SARS-CoV-2 using
232 the tools which were state of the art, we deeply analyzed the host likelihood profiles of
233 viruses output by DeepHoF to seek specific vertebrate hosts of the early-stage SARS-
234 CoV-2 isolates. In this study, we proposed that viruses with the same host species
235 possessed the host likelihood score profiles close in the five-dimensional space. Based
236 on this assumption, we compared the host likelihood score profile of SARS-CoV-2 with
237 those of the non-human vertebrate viruses released in GenBank [29] before the
238 pandemic outbreak of SARS-CoV-2 (Methods). We found that minks (*Mustela*
239 *lutreola/Neovison vison*) were the most probable host, followed by Chinese rufous
240 horseshoe bats (*Rhinolophus sinicus*), dogs (*Canis lupus familiaris*), Pomona roundleaf
241 bats (*Hipposideros Pomona*) and cat family (*Felidae*) (**Table 2**, Supplemental Table S3).
242 In contrast, minks, Chinese rufous horseshoe bats, dogs and cat family were
243 respectively classified into very low, low or medium groups by Damas *et al.*, [10], who
244 divided 410 vertebrate species into five categories from very high to very low
245 depending on the susceptibility to SARS-CoV-2 based on the analysis of sequence
246 similarity of ACE2 and protein structure of ACE2/SARS-CoV-2 S-binding interface
247 from the vertebrates. In the later world-wide pandemic, it should be pointed out that all
248 the probable hosts we predicted were proved by animal experiments or the infection
249 events [5], which illustrated the usefulness of such analysis for the host inference of
250 SARS-CoV-2. Remarkably, SARS-CoV-2 has been reported largely to infect farmed
251 minks in Netherlands, Denmark, Spain, the United States, Sweden, Italy, Greece,
252 France, Lithuania, Canada, and Poland from April to February, 2021. As of February, 2021,
253 SARS-CoV-2 had been reported to sweep 69 and 207 mink farms in Netherlands and
254 Denmark, respectively, which accelerated the cull of minks and killed the fur industry
255 in the two countries. On 9 October, 2020, at least 10,000 minks were reported dead at
256 Utah and Wisconsin mink farms in the USA, and they were believed infected by SARS-
257 CoV-2 [5] (Table 2).

258 When evaluating the contributions of 11 genes of SARS-CoV-2 in determining
259 mink as the most probable host, we found ORF1ab and ORF8 contributed the most

260 (Supplemental Table S4), which suggesting that genes show different contributions
261 when determining different hosts. The rationality of this result is supported by the roles
262 of ORF1ab in viral replication and host survival [27], and the roles of ORF8 related to
263 immune evasion [30]. However, the interaction between the two genes and the mink
264 cell should merit the further attention and investigation.

265 Additionally, novel coronaviruses, which possess high sequence similarity with
266 SARS-CoV-2, were found on pangolin [2, 3] in China. Even though these pangolin-
267 associated coronaviruses were assigned similar host likelihood score profiles with
268 early-stage SARS-CoV-2 isolates, our analysis demonstrated that the similarity of
269 profiles between SARS-CoV-2 and pangolin-associated coronaviruses was lower than
270 those between SARS-CoV-2 and certain viruses of mink and Chinese rufous horseshoe
271 bat.

272 **Association of SARS-CoV-2 between humans and minks**

273 In April 2020, farmed minks in Netherlands were noticed to be infected by SARS-CoV-
274 2 because of the abnormal mortality [4]. Even though all the mink farms in Netherlands
275 have been screened mandatorily since 28 May 2020, the transmission of coronavirus
276 among the mink population did not seem to cease. Thus, a million farmed minks were
277 culled in Netherlands, and followed by a plan to cull 2.5 million farmed minks in
278 Denmark.

279 Characterizing SARS-CoV-2 by their host likelihood score profiles, we found the
280 isolates detected on humans and minks in Netherlands distributed in a consistent mode,
281 where both groups were divided into a major cluster and a divergence (Figure 3D, 1,746
282 SARS-CoV-2 samples collected from humans in Netherlands as of September 15 and
283 153 SARS-CoV-2 samples collected from farmed minks in Netherlands as of October
284 15 were used respectively, Methods). For SARS-CoV-2, as the host likelihood score on
285 susceptible hosts such as human and mink can also indicate the likelihood to infect
286 these animals, the mode of host likelihood score profile can reflect its property of viral
287 infection. Consequently, the consistency mentioned above hinted the close infection-

288 related behaviors of SARS-CoV-2 on humans and minks in Netherlands and thus
289 illustrated the association of SARS-CoV-2 isolates collected from the two populations.
290 Furthermore, nine of 14 high-frequency variants in human-derived SARS-CoV-2
291 genomes sequenced in Netherlands were absent in the genomes detected in other
292 countries. Herein we used NC_045512 as the reference for variant calling, regarded the
293 variants with $\geq 5\%$ frequency as high-frequency ones and filtered out the synonymous
294 single nucleotide polymorphisms (SNPs) (Supplemental Table S5). Among these
295 unique high-frequency variants in Dutch human-derived SARS-CoV-2, two were found
296 in Dutch mink-derived SARS-CoV-2, thus proved the circulation of SARS-CoV-2
297 between humans and minks in Netherlands. It was remarkable that our findings could
298 be supported by the conclusions from a research team in Netherland, who utilized more
299 detailed information about patients and related mink farms [12]. In the 2020 world-
300 wide pandemic, minks are the only animal that has been reported to transmit SARS-
301 CoV-2 to humans [11, 12]. We further compared the high-frequency variants of SARS-
302 CoV-2 isolates in humans and minks in Netherlands. Except for four common variants,
303 SARS-CoV-2 isolates derived from minks still had 23 unique high-frequency variants
304 and six were found on S protein that is related to virus-host fusion process. This result
305 indicated that the virus might have gained higher diversity after the intra-species
306 circulation among mink herd and inter-species circulation between minks and human.
307 As the mink infections are expanding worldwide, the association and circulation of
308 SARS-CoV-2 between humans and minks in Netherlands notifies us of the importance
309 to take precautions of the bidirectional transmission in other regions.

310 **Retrospective analysis of the world-wide pandemic**

311 To verify the stability and uniformity of the host inference among SARS-CoV-2
312 samples, retrospective analysis of more isolates in the lasting pandemic was required.
313 As the surge in variants of SARS-CoV-2 complicated the host prediction of the novel
314 virus, we utilized 102,804 SARS-CoV-2 genomes released on GISAID EpiCoV
315 Database (<https://www.gisaid.org/>) [31] as of 15 September 2020, before the rapid
316 accumulation of mutations in SARS-CoV-2. We picked out 53,759 genomes which met

317 the quality standard given by Chinese Academy of Sciences [32] and trimmed their
318 varied-length 5'- and 3'-untranslated regions (UTR) based on the annotation of
319 NC_045512 (Methods). We calculated the host likelihood score profiles of the 53,759
320 isolates (Supplemental Table S5) and conducted principal component analysis (PCA)
321 on the profiles. As shown in **Figure 4A**, we found a clear cluster of all SARS-CoV-2
322 isolates with 17 earliest ones locating in the center. The kernel density estimation curves
323 displayed on the first two principal components were approximately normally
324 distributed. As the profiles of the 53,759 isolates are under the normal distribution
325 mentioned above, the host range of SARS-CoV-2 isolates keep consistent throughout
326 the pandemic and it is therefore reasonable that the validity of the host inference using
327 the earliest 17 isolates would be efficient in the later pandemic.

328 However, when the SARS-CoV-2 isolates were divided chronologically using 15
329 April 2020 as the split date, which divided 53,759 isolates into two parts more evenly
330 than other dates, we found that the two subsets have divergent distributions in each of
331 the two dimensions of PCA (two-sided two-sample Kolmogorov-Smirnov test, *p*-value
332 = 0, *n*_{isolates} = 26,167 before 15 April 2020 and 27,592 after 15 April 2020) (Figure 4B).
333 The approximately normal distribution of SARS-CoV-2 genomes and their time-
334 dependent feature indicate the overall consistency and a certain extent of divergence in
335 the host likelihood score profiles of SARS-CoV-2 isolates.

336 To explain the divergence among host likelihood score profiles, we identified all
337 variants in 53,759 genomes (Supplemental Table S5). The 13 high-frequency variants
338 were located on S gene, N gene, ORF1ab, ORF8 and ORF3a, some of which are related
339 to virus-host fusion process [22, 33]. Furthermore, we annotated our PCA result with
340 the GISAID nomenclature system [31] which divides all SARS-CoV-2 genomes into
341 six major clades based on marker variants that appeared over time. Most of the marker
342 variants were recognized as high-frequency variants in the variant calling. As we can
343 see in Figure 4C, SARS-CoV-2 isolates fell into several clear fusiform clusters
344 according to their clades. This indicated that those marker variants might explain the
345 divergence among host likelihood score profiles. When we manually mutated the 17

346 earliest sequenced genomes with those marker variants, we found the variants marking
347 each clade drove the earliest sequenced SARS-CoV-2 to the corresponding cluster of
348 the clade (Supplemental Figure S4), which verified our previous speculation and
349 demonstrated the efficacy of DeepHoF to identify the important variants emerging in
350 the virus's evolution. However, as the consistency of the distribution of host likelihood
351 score profiles were not disturbed, it hinted that these mutations did not change the host
352 range of SARS-CoV-2.

353 Furthermore, to explore the trend of host likelihood of the SARS-CoV-2 over time,
354 we finally examined the relationships between sampling time and the host likelihood
355 scores on non-human vertebrates and humans (Figure 4D). We found that both scores
356 gradually descended. As the host likelihood scores on susceptible hosts also indicate
357 the likelihood to be infected by SARS-CoV-2 from a computational point of view, the
358 trends might indicate the gradually descending infectiousness to human and other
359 vertebrates from the outbreak to 15 September 2020. Those trends may not be so
360 pronounced, but they should arouse our attention.

361

362 **Discussion**

363 In summary, we proposed a deep learning method, DeepHoF, based on extracting the
364 viral genomic features, to calculate the host likelihood scores on five host types.
365 DeepHoF made up for the vacancy of a universal tool feasible to any novel virus. For
366 the identification of five host types, our model can significantly outperform BLAST
367 and well discriminate the human-infecting and non-human-infecting viruses like
368 coronaviruses. Overcoming the limitation of sequence similarity-based methods to
369 disclose the host information of novel viruses, DeepHoF demonstrated the practicality
370 to SARS-CoV-2 in the 2020 pandemic. Using 17 SARS-CoV-2 isolates sequenced in
371 the earliest stage of COVID-19 detection, DeepHoF evaluated the host likelihood
372 scores on humans and non-human vertebrates for SARS-CoV-2. Filling the gap in
373 predicting the host species for any novel virus that remained unsolved using the tools
374 which were state of the art, we further analyzed the host likelihood score profile to

375 further infer the specific hosts of SARS-CoV-2. The hosts determined by DeepHoF can
376 be either reservoirs or susceptible middle hosts, which are not discriminated in this
377 study. We found minks, bats, dogs and cats could be potential hosts of SARS-CoV-2,
378 while minks might be one of the most noteworthy animal hosts. Due to mutations, the
379 host likelihood score profiles of the isolates in the long period of the later pandemic had
380 slightly varied, but followed normal distribution where those of the early 17 isolates
381 locate in the center. As a consequence, the host range inferred with the profiles of the
382 isolates during the pandemic was consistent with the inference using the early samples.
383 Additionally, based on the model, we further found three genes (S gene, ORF7b and
384 ORF1ab) and two genes (ORF1ab and ORF8) were significant in determining the host
385 likelihood score on human and the host range for SARS-CoV-2, respectively. The genes
386 involving virus-host fusion process (S gene), viral replication (ORF1ab) and host
387 survival (ORF1ab) played a significant role in determining human as the host, while
388 the genes related to viral replication (ORF1ab), host survival (ORF1ab) and immune
389 evasion (ORF8) were significant to determine the host range for SARS-CoV-2. For the
390 prevention and control of a novel epidemic disease such as COVID-19, the prediction
391 of probable hosts is essential at the early stage of the epidemic outbreak. In view of this,
392 our study is expected to play a potentially effective role in support of those efforts.

393 Furthermore, according to the analysis results of host likelihood score profiles of
394 humans and minks in Netherlands, we found a strong association of SARS-CoV-2
395 isolates collected from the two populations and disclosed the contribution of mink on
396 higher divergence in SARS-CoV-2. The phenomenon coincided with the analysis result
397 of variant calling and could be explained by characteristics of minks in virus circulation.
398 As reported by previous studies about avian-derived influenza A virus, minks serve as
399 a significant node in the viral transmission network, connecting animals from different
400 families and acting as domesticators for viral adaptation to mammals [34]. As the only
401 one animal that has been reported to transmit SARS-CoV-2 to humans, the role of minks
402 in the evolution of SARS-CoV-2 should be studied in depth. Therefore, with a large-
403 scale genome analysis based on DeepHoF's computation for the later world-wide

404 pandemic, it should not be slighted for the relationship of SARS-CoV-2 between
405 humans and minks.

406 Although we have applied DeepHoF to SARS-CoV-2 in the current study, the
407 application of DeepHoF is not limited to this virus. DeepHoF is also feasible to
408 determine the host ranges for many other novel viruses, such as the small circular rep-
409 encoding ssDNA viruses newly discovered on wild animals and domestic animals or in
410 the environment. However, limitations of DeepHoF lie in that it does not consider the
411 host sequence information, which can be improved in the future. DeepHoF also does
412 not discriminate between reservoir hosts, vector hosts and other susceptible hosts.
413 Meanwhile, the present study is expected to be further confirmed with both the ongoing
414 events of pandemic and additional experimental findings, and the interpretation of our
415 analysis should be still kept a certain caution.

416 Represented by SARS-CoV-2, more complex and larger numbers of viral genome
417 data will be produced in similar epidemics in the future. In addition, the metagenome
418 and the metavirome can also be used in the prevention and control of the epidemic. The
419 United States Agency for International Development launched the Global Virus
420 Program in 2018 to reduce possible epidemiological threats by studying metaviromic
421 samples from more than 35 countries around the world [35]. It is estimated that there
422 are about 1.67 million novel viruses in mammals, birds and other important hosts of
423 zoonotic viruses. Among them, 631,000-827,000 have the potential to cause zoonotic
424 diseases [35]. However, only 263 viruses from 25 virus families have been confirmed
425 to infect humans [36]. Newly emerged infectious viruses keep threatening our health
426 and well-being. Under the circumstances, using computational methods to discover
427 pathogenetic viruses and acquire knowledge, including the host range, about novel
428 viruses can provide timely response in the prevention of epidemics and pandemics. In
429 the future, the detection of novel viruses will rely more heavily on high-throughput
430 sequencing technologies such as metagenomics and metaviromics. Thus, more robust
431 tools designed for metagenomes and metaviromes are required.

432

433 **Materials and Methods**

434 **Datasets construction for training and test**

435 We downloaded 63,049 whole viral genomes from GenBank by 9 July, 2019, and
436 tagged them with five host labels (plant, germ, invertebrate, non-human vertebrate and
437 human), which were integrated from the host metadata provided by GenBank
438 (Supplemental Table S6). The five host types covered all the living organism hosts. For
439 viruses infecting multiple host types, multiple labels were given. Following the data
440 collection procedure, short fragments were generated randomly from those tagged
441 whole genomes because of the computational cost in long sequence processing. The
442 training set was constructed with short fragments from 55,283 genomes released before
443 1 January, 2018, and the test set was constructed with the rest (the Accession list and
444 the host information of the genomes used for training and test are in Supplemental Table
445 S7). There is non-overlap of virus species in the training and test sets.

446 **Mathematical representation of viral whole genomes**

447 Due to the long-term adaptation to natural reservoirs, viruses share some evolutionary
448 signatures in nucleotide sequences, such as codon pair, dinucleotide, codon, and amino
449 acid biases, with their natural reservoirs [15]. Besides, viral proteins, especially the
450 receptors that are effectively attached to the host cell membrane, are crucial factors for
451 viruses to invade and infect the host cells [37]. In brief, the genome compositions of
452 viruses can inform host-virus correlation.

453 Herein, we represent a given viral sequence with a base one-hot matrix (BOH) and
454 a codon one-hot matrix (COH), digitizing the genetic information of the virus on
455 nucleotide and codon level respectively. To start with, bases and codons are encoded
456 with one-hot format to work with deep learning algorithms. In the coding of BOH, each
457 consecutive base of a query sequence linked by its complementary strand is encoded
458 by one-hot. For COH, we do not extract ORFs since coding sequences make up most
459 of the viral genome. Instead, we directly concatenate the six phases of the input
460 sequence (Supplemental Figure S5), and then each consecutive codon of the joined
461 sequences is encoded by one-hot. Consequently, for an input sequence of length L, it

462 will be transformed to a BOH matrix, with the size of $2L \times 4$, and a COH matrix, with
463 the size of $2L \times 64$.

464 **BiPathCNN Model descriptions**

465 In building the framework of DeepHoF, we firstly utilize a BiPathCNN [38], containing
466 two CNN paths, digging information from the BOH matrix and COH matrix
467 respectively. The information is naturally corresponding to the viral genomic features
468 for the viruses which infect the same kind of hosts. After independent convolution and
469 pooling operations at the beginning, the two paths are combined by a concatenation
470 layer. Following a normalization layer, five prediction scores will be provided by five
471 sub-paths, containing five independent nodes, corresponding to five independent binary
472 classifications on plant, germ, invertebrate, non-human vertebrate and human
473 individually, in the output layer with sigmoid activation and binary cross-entropy loss
474 function for each node. The architecture of DeepHoF is shown in Supplemental Figure
475 S6 and the details of each layer in BiPathCNN are described in Supplementary
476 Information.

477 **Implementation of DeepHoF**

478 In the practical application, viral nucleotide sequence is the only input required by
479 DeepHoF. For a viral whole genome sequence (or a partial genome sequence), a cut
480 window moves along the long sequence without overlapping to separate it into suitable
481 fragments for the pre-trained BiPathCNN model. DeepHoF firstly predicts the host
482 infection scores for each fragment. Then it calculates the final score by weighting and
483 summing the predicted scores of each fragment. For example, a 2,000 bp query
484 sequence is separated into three consecutive fragments, corresponding to the first 800
485 bp, the middle 800 bp and the last 400 bp of the query sequence. Then DeepHoF
486 predicts the three fragments independently and calculates the weighted average of the
487 three predicted score vectors with the weights of $800/2,000$, $800/2,000$, and $400/2,000$
488 respectively. For each input sequence, DeepHoF outputs five scores on five host types,
489 respectively. Besides, DeepHoF provides the *p*-values of each score, statistically
490 measuring of how distinct the scores are compared with those of non-infectious viruses

491 [22]. For example, if an input virus has a score of 0.4 on human, we compare 0.4 with
492 the scores of non-human viruses in our dataset and provide the *p*-value as a judgment
493 basis. If the *p*-value is less than 0.05, we conclude that human is the probable host of
494 the input virus with a significantly higher score on human host type than non-human
495 viruses.

496 As the host likelihood score profile of a virus, consisting of the five predicted scores
497 given by DeepHoF, can be regarded as a host-related feature vector extracted by
498 DeepHoF, we utilize it to characterize the virus. It is logistical to regard the viruses with
499 the same host species possess the similar host likelihood score profiles. Based on this
500 assumption, the potential host species of a virus can be inferred by the analysis of the
501 profiles. To quantitatively compare host likelihood score profiles between viruses, we
502 calculated the Euclidean distance between the profiles. In the case of SARS-CoV-2, we
503 searched the detailed vertebrate host of the earliest detected isolates, which are closer
504 to the most recent common ancestor of SARS-CoV-2. To start with, we added the host
505 annotations provided by Virus-Host DB [39] to the vertebrate viruses included in
506 GenBank. Here, the average of host likelihood score profiles of 17 earliest sequenced
507 isolates was used as the representation of SARS-CoV-2. We calculated the Euclidean
508 distance between the profile of SARS-CoV-2 and that of each non-human vertebrate
509 virus (discovered before the outbreak of SARS-CoV-2). We regarded the vertebrate
510 infected by a virus possessing profile close to that of SARS-CoV-2 was the probable
511 host of SARS-CoV-2.

512 **Data filtering and trimming for SARS-CoV-2 genome sequences**

513 There were 102,804 SARS-CoV-2 genomes released on GISAID EpiCoV Database as
514 of 15th September 2020. We downloaded all the sequences and filtered them with the
515 quality standard given by the Chinese Academy of Sciences [32]. Because the UTRs
516 were not taken as seriously as the protein-coding regions and the lengths of sequenced
517 UTRs varied a lot in different SARS-CoV-2 genomes, we trimmed the 5'- and 3'- UTR
518 according to the annotation of NC_045512 to get rid of noises. Thus, we finally got
519 53,759 clean sequences.

520 **Phylogenetic analysis and single nucleotide polymorphisms analysis**

521 In this study, we applied Clustal Omega software [40] (version 1.2.4) for multiple
522 sequence alignment and RAxML software [41] (version 8.2.12) for phylogenetic tree
523 building using maximum likelihood methods with 1000 bootstrap replicates. Snippy
524 [42] (version 4.4.3) was utilized for variant calling, using NC_045512 as the reference
525 genome. In this study, we filtered out the synonymous SNPs and regarded the variants
526 with $\geq 5\%$ frequency as high-frequency ones. Commands of the three tools are
527 included in Supplementary Information.

528

529 **Authors' contributions**

530 HQZ and YHX co-supervised the study. QG, ML, CHW, JYG, XQJ and HQZ
531 developed the DeepHoF model, conducted the analyses and wrote the manuscript. HQZ
532 and ZCF helped with designing the model. MZ calculated performance metrics of
533 DeepHoF and BLAST. PHW helped with phylogeny analysis and SNP analysis. JT,
534 SFW and TTX made plots and table for the results. All authors read and approved the
535 final manuscript.

536

537 **Competing interests**

538 The authors have declared no competing interests.

539

540 **Acknowledgements**

541 We acknowledge GISAID (<https://www.gisaid.org/>) for facilitating open data sharing.
542 This work was supported by the National Key Research and Development Program of
543 China (2017YFC1200205) and the National Natural Science Foundation of China
544 (32070667, 31671366). Part of the analysis was performed on the High Performance
545 Computing Platform of the Center for Life Science of Peking University.

546

547 **References**

548 [1] Zhou P, Yang X-L, Wang X-G, Hu B, Zhang L, Zhang W, et al. A pneumonia
549 outbreak associated with a new coronavirus of probable bat origin. *nature*
550 2020;579:270-3.

551 [2] Lam TT-Y, Jia N, Zhang Y-W, Shum MH-H, Jiang J-F, Zhu H-C, et al. Identifying
552 SARS-CoV-2-related coronaviruses in Malayan pangolins. *Nature* 2020;583:282-5.

553 [3] Xiao K, Zhai J, Feng Y, Zhou N, Zhang X, Zou J-J, et al. Isolation of SARS-CoV-
554 2-related coronavirus from Malayan pangolins. *Nature* 2020;583:286-9.

555 [4] Oreshkova N, Molenaar RJ, Vreman S, Harders F, Munnink BBO, Hakze-van Der
556 Honing RW, et al. SARS-CoV-2 infection in farmed minks, the Netherlands, April and
557 May 2020. *Eurosurveillance* 2020;25:2001005.

558 [5] OIE. COVID-19 Portal: Events in Animals. <https://www.oie.int/en/scientific-expertise/specific-information-and-recommendations/questions-and-answers-on-2019novel-coronavirus/events-in-animals/> (Oct 25 2020, date last accessed).

559 [6] Shi J, Wen Z, Zhong G, Yang H, Wang C, Huang B, et al. Susceptibility of ferrets,
560 cats, dogs, and other domesticated animals to SARS–coronavirus 2. *Science*
561 2020;368:1016-20.

562 [7] Sia SF, Yan L-M, Chin AW, Fung K, Choy K-T, Wong AY, et al. Pathogenesis and
563 transmission of SARS-CoV-2 in golden hamsters. *Nature* 2020;583:834-8.

564 [8] Munster VJ, Feldmann F, Williamson BN, Van Doremalen N, Pérez-Pérez L, Schulz
565 J, et al. Respiratory disease in rhesus macaques inoculated with SARS-CoV-2. *Nature*
566 2020;585:268-72.

567 [9] Santini JM, Edwards SJ. Host range of SARS-CoV-2 and implications for public
568 health. *The Lancet Microbe* 2020;1:e141-e2.

569 [10] Damas J, Hughes GM, Keough KC, Painter CA, Persky NS, Corbo M, et al. Broad
570 host range of SARS-CoV-2 predicted by comparative and structural analysis of ACE2
571 in vertebrates. *Proceedings of the National Academy of Sciences* 2020;117:22311-22.

572 [11] Mallapaty S. What's the risk that animals will spread the coronavirus. *Nature* 2020.

575 [12] Munnink BBO, Sikkema RS, Nieuwenhuijse DF, Molenaar RJ, Munger E,
576 Molenkamp R, et al. Transmission of SARS-CoV-2 on mink farms between humans
577 and mink and back to humans. *Science* 2021;371:172-7.

578 [13] Guo Q, Li M, Wang C, Wang P, Fang Z, tan J, et al. Host and infectivity prediction
579 of Wuhan 2019 novel coronavirus using deep learning algorithm. *bioRxiv*
580 2020:2020.01.21.914044.

581 [14] Rothenburg S, Brennan G. Species-specific host–virus interactions: implications
582 for viral host range and virulence. *Trends in microbiology* 2020;28:46-56.

583 [15] Babayan SA, Orton RJ, Streicker DG. Predicting reservoir hosts and arthropod
584 vectors from evolutionary signatures in RNA virus genomes. *Science* 2018;362:577-80.

585 [16] Lu G, Wang Q, Gao GF. Bat-to-human: spike features determining ‘host jump’ of
586 coronaviruses SARS-CoV, MERS-CoV, and beyond. *Trends in microbiology*
587 2015;23:468-78.

588 [17] Li W, Zhang C, Sui J, Kuhn JH, Moore MJ, Luo S, et al. Receptor and viral
589 determinants of SARS-coronavirus adaptation to human ACE2. *The EMBO journal*
590 2005;24:1634-43.

591 [18] Villarroel J, Kleinheinz KA, Jurtz VI, Zschach H, Lund O, Nielsen M, et al.
592 HostPhinder: a phage host prediction tool. *Viruses* 2016;8:116.

593 [19] Galiez C, Siebert M, Enault F, Vincent J, Söding J. WIsh: who is the host?
594 Predicting prokaryotic hosts from metagenomic phage contigs. *Bioinformatics*
595 2017;33:3113-4.

596 [20] Gałan W, Bąk M, Jakubowska M. Host taxon predictor-a tool for predicting taxon
597 of the host of a newly discovered virus. *Scientific reports* 2019;9:1-13.

598 [21] Mock F, Viehweger A, Barth E, Marz M. VIDHOP, viral host prediction with deep
599 learning. *Bioinformatics* 2020.

600 [22] Ren J, Ahlgren NA, Lu YY, Fuhrman JA, Sun F. VirFinder: a novel k-mer based
601 tool for identifying viral sequences from assembled metagenomic data. *Microbiome*
602 2017;5:1-20.

603 [23] Belouzard S, Millet JK, Licitra BN, Whittaker GR. Mechanisms of coronavirus
604 cell entry mediated by the viral spike protein. *Viruses* 2012;4:1011-33.

605 [24] Brister JR, Ako-Adjei D, Bao Y, Blinkova O. NCBI viral genomes resource.
606 *Nucleic acids research* 2015;43:D571-D7.

607 [25] Li Y-H, Hu C-Y, Wu N-P, Yao H-P, Li L-J. Molecular characteristics, functions,
608 and related pathogenicity of MERS-CoV proteins. *Engineering* 2019;5:940-7.

609 [26] Cheng VC, Lau SK, Woo PC, Yuen KY. Severe acute respiratory syndrome
610 coronavirus as an agent of emerging and reemerging infection. *Clinical microbiology*
611 *reviews* 2007;20:660-94.

612 [27] Hu B, Guo H, Zhou P, Shi Z-L. Characteristics of SARS-CoV-2 and COVID-19.
613 *Nature Reviews Microbiology* 2020:1-14.

614 [28] Wong L-YR, Ye Z-W, Lui P-Y, Zheng X, Yuan S, Zhu L, et al. Middle East
615 Respiratory Syndrome Coronavirus ORF8b Accessory Protein Suppresses Type I IFN
616 Expression by Impeding HSP70-Dependent Activation of IRF3 Kinase IKK ϵ . *The*
617 *Journal of Immunology* 2020;205:1564-79.

618 [29] Sayers EW, Cavanaugh M, Clark K, Pruitt KD, Schoch CL, Sherry ST, et al.
619 GenBank. *Nucleic acids research* 2021;49:D92-D6.

620 [30] Young BE, Fong S-W, Chan Y-H, Mak T-M, Ang LW, Anderson DE, et al. Effects
621 of a major deletion in the SARS-CoV-2 genome on the severity of infection and the
622 inflammatory response: an observational cohort study. *The Lancet* 2020;396:603-11.

623 [31] Shu Y, McCauley J. GISAID: Global initiative on sharing all influenza data—from
624 vision to reality. *Eurosurveillance* 2017;22:30494.

625 [32] Zhao W-M, Song S-H, Chen M-L, Zou D, Ma L-N, Ma Y-K, et al. The 2019 novel
626 coronavirus resource. *Yi chuan = Hereditas* 2020;42:212-21.

627 [33] Lan J, Ge J, Yu J, Shan S, Zhou H, Fan S, et al. Structure of the SARS-CoV-2 spike
628 receptor-binding domain bound to the ACE2 receptor. *Nature* 2020;581:215-20.

629 [34] Xue R, Tian Y, Hou T, Bao D, Chen H, Teng Q, et al. H9N2 influenza virus isolated
630 from minks has enhanced virulence in mice. *Transboundary and emerging diseases*
631 2018;65:904-10.

632 [35] Carroll D, Daszak P, Wolfe ND, Gao GF, Morel CM, Morzaria S, et al. The global
633 virome project. *Science* 2018;359:872-4.

634 [36] King AM, Lefkowitz E, Adams MJ, Carstens EB. Virus taxonomy: ninth report of
635 the International Committee on Taxonomy of Viruses. Elsevier, 2011.

636 [37] Dimitrov DS. Virus entry: molecular mechanisms and biomedical applications.
637 *Nature Reviews Microbiology* 2004;2:109-22.

638 [38] Fang Z, Tan J, Wu S, Li M, Xu C, Xie Z, et al. PPR-Meta: a tool for identifying
639 phages and plasmids from metagenomic fragments using deep learning. *Gigascience*
640 2019;8:giz066.

641 [39] Mihara T, Nishimura Y, Shimizu Y, Nishiyama H, Yoshikawa G, Uehara H, et al.
642 Linking virus genomes with host taxonomy. *Viruses* 2016;8:66.

643 [40] Sievers F, Wilm A, Dineen D, Gibson TJ, Karplus K, Li W, et al. Fast, scalable
644 generation of high-quality protein multiple sequence alignments using Clustal Omega.
645 *Molecular systems biology* 2011;7:539.

646 [41] Stamatakis A. RAxML-VI-HPC: maximum likelihood-based phylogenetic
647 analyses with thousands of taxa and mixed models. *Bioinformatics* 2006;22:2688-90.

648 [42] Seemann T. Snippy: rapid bacterial SNP calling and core genome alignments.
649 <https://github.com/tseemann/snippy.git> (Oct 25 2020, date last accessed).

650 [43] Letunic I, Bork P. Interactive Tree Of Life (iTOL) v4: recent updates and new
651 developments. *Nucleic acids research* 2019;47:W256-W9.

652

653 **Figure legends**

654 **Figure 1 DeepHoF outperforms BLAST and well learns the information of virus
655 hosts**

656 **A.** Average ROC curves and AUC values of DeepHoF and BLAST. DeepHoF performs
657 better than BLAST on average AUC of five host types. **B.** Comparison of host
658 likelihood scores predicted by DeepHoF between human-infecting and non-human-
659 infecting coronaviruses on human. The former performed higher probabilities than the
660 latter (two-sided unpaired Welch Two Sample *t*-test, $t_{(43.843)} = 8.265$ and $t_{(38.016)} = 4.674$,

661 p -values = 1.732×10^{-10} and 3.657×10^{-5} . *** p -value < 0.0001, t -values and degrees of
662 freedom were presented as $t_{(df)}$. **C.** Phylogenetic analyses of whole genomes of
663 coronaviruses. **D.** Phylogenetic analyses of S genes of coronaviruses. Maximum-
664 likelihood phylogenetic trees were built by RAxML [41] with 1,000 bootstrap replicates
665 and visualized with iTOL [43]. The whole genomes and the S genes of the human-
666 infecting coronaviruses could not be distinguished from the non-human-infecting ones.
667 (Red: human-infecting coronaviruses; Blue: non-human-infecting coronaviruses).

668 **Figure 2 The workflow of application of DeepHoF on NC_045512**

669 In the application of DeepHoF on SARS-CoV-2 NC_045512, the whole genome of
670 NC_045512 was the only input required by the pre-trained DeepHoF model and coded
671 into BOH and COH matrix for BiPathCNN network. DeepHoF output the host
672 likelihood scores of NC_045512 on five host types respectively and the corresponding
673 significance. The hosts of NC_045512 were predicted to be non-human vertebrates and
674 humans with p -values less than 0.05. Simultaneously, NC_045512 was characterized
675 by its host likelihood score profile. Susceptible to viruses with similar profile, *Mustela*
676 *lutreola/ Neovison vison*, *Rhinolophus sinicus*, *Canis lupus familiaris*, *Hipposideros*
677 *pomona* and Feline were output as the probable hosts of NC_045512. BOH: base one-
678 hot matrix, COH: codon one-hot matrix.

679 **Figure 3 Evaluation of host likelihood scores of SARS-CoV-2**

680 The contribution of each gene in the prediction and the visualization of host likelihood
681 score profiles of SARS-CoV-2 isolates sampled in Netherlands. **A.** Host likelihood
682 scores of 17 earliest detected SARS-CoV-2 isolates and other coronaviruses on humans
683 and non-human vertebrates. SARS-CoV-2 showed high host likelihood scores on both
684 humans and non-human vertebrates with p -values less than 0.05. In addition, SARS-
685 CoV-2 was predicted lower score than SARS-CoV and comparable score to MERS-
686 CoV on human. As for host likelihood scores on non-human vertebrates, SARS-CoV-
687 2, SARS-CoV and MERS-CoV were close to each other. Host likelihood scores have
688 p -values less than 0.05 are marked 'Y (yes)'. (Red: human-infecting coronaviruses; *:
689 the 17 earliest collected SARS-CoV-2 isolates). **B.** Hierarchical clustering of early-

690 stage SARS-CoV-2 and other coronaviruses using five-dimensional host likelihood
691 score profiles given by DeepHoF. The profile of SARS-CoV-2 was close to that of
692 SARS-CoV and MERS-CoV (Red: SARS-CoV-2; Blue: SARS-CoV; Yellow: MERS-
693 CoV). **C.** Contributions of the protein coding genes on determining the host likelihood
694 scores of SARS-CoV-2, SARS-CoV and MERS-CoV on human. The structural genes,
695 ORF1ab and group-specific genes contributed differently in the three coronaviruses
696 (two-sided unpaired Welch Two Sample t-test, p -value < 0.05, see in Supplemental
697 Figure S3). S, ORF7b and ORF1ab were the most pivotal in SARS-CoV-2. ORF7b,
698 ORF9b and S were the most considerable in SARS-CoV. ORF8b, N and ORF3
699 contributed the most in MERS-CoV (S: spike glycoprotein coding gene; M:
700 membrane/matrix glycoprotein coding gene; N: nucleocapsid phosphoprotein coding
701 gene; E: envelope coding gene). **D.** Principal component analysis (PCA) of host
702 likelihood score profiles of SARS-CoV-2 detected on humans and minks in Netherlands.
703 The host likelihood score profiles of mink-derived and human-derived SARS-CoV-2
704 isolates in Netherlands are distributed in a consistent mode, containing a major cluster
705 and divergence. The host likelihood score profiles of human-derived (left) and mink-
706 derived (right) SARS-CoV-2 isolates in Netherlands distributed in a consistent mode,
707 both containing a major cluster (red) and divergence (blue). The major cluster and the
708 divergence were divided by the pam function of R package cluster.

709 **Figure 4 Entirety and divergence in the host likelihood score profiles of 53,759
710 SARS-CoV-2 isolates in the later world-wide pandemic**

711 **A.** PCA of host likelihood score profiles of 53,759 SARS-CoV-2 isolates and the
712 distribution on each principal component. All the host s likelihood core profiles of
713 53,759 SARS-CoV-2 isolates were clustered with 17 earliest sequenced isolates located
714 in the center and the density curves displayed on each principal component were
715 approximate normal distribution. **B.** Distributions of host likelihood score profiles of
716 53,759 SARS-CoV-2 isolates collected before and after 15 April 2020. When the
717 SARS-CoV-2 isolates were divided chronologically using 15 April 2020 as the split
718 date, which divided the 53,759 isolates into two parts more evenly than other dates. The

719 host likelihood score profiles of SARS-CoV-2 before and after 15 April 2020 had
720 divergent distributions on each principal component (two-sided two-sample
721 Kolmogorov-Smirnov test, p -value = 0, $n_{isolates}$ = 26,167 before 15 April 2020 and
722 27,592 after 15 April 2020. Blue, 26,167 isolates collected before 15 April 2020; Red,
723 27,592 isolates collected after 15 April 2020; Grey, all the 53,759 isolates). **C.** GISAID
724 clades represented in PCA of host likelihood score profiles of 53,759 SARS-CoV-2
725 genomes. All the 53,759 samples representing 53,759 host likelihood score profiles
726 were painted with six different colours corresponding to six different GISAID clades
727 of SARS-CoV-2. SARS-CoV-2 isolates fell into several clear fusiform clusters with
728 different colours according to their clades. **D.** Time series of the host likelihood scores
729 on humans and non-human vertebrates for SARS-CoV-2 in the later world-wide
730 pandemic. The host likelihood scores on humans and non-human vertebrates descend
731 gradually with time (linear regression model analysis, R -squared = 6.806×10^{-3} and
732 1.431×10^{-2} , $t_{(53,757)} = -19.22$ and $t_{(53,757)} = -27.96$, p -values = 5.543×10^{-84} and
733 3.292×10^{-272} , slopes = -1.853×10^{-6} and -3.768×10^{-6}).

734

735 **Tables**

736 **Table 1 Performance metrics of DeepHoF and BLAST**

Methods	Precision	Accuracy	TPR	FPR	AUC	F1-score
BLAST	0.699	0.892	0.888	0.107	0.833	0.896
DeepHoF	0.968	0.964	0.865	0.008	0.987	0.963

737 TPR: true-positive rate; FPR: false-positive rate; AUC: area under the curve

738

Table 2 Host prediction results of SARS-CoV-2

Prediction	Evidence of infection with SARS-CoV-2 [5]	Reported
		transmission to humans



Mustela lutreola
/Neovison vison

- From 19 April to 1 October, 2020, out of around 120 mink farms in Netherlands, 57 have been declared infected;
- From 17 June to 1 October, 2020, SARS-CoV-2 has been detected in 41 mink farms in Denmark;
- On 16 July, 2020, 80% of the animal samples were tested positive in a Spanish farm;
- On 17 August, 2020, confirmed cases were reported in minks at two farms in Utah, the United States;
- On 9 October, 2020, 10,000 minks were dead at the United States fur farms and believed infected by SARS-CoV-2.

- Two cases that minks transmitted SARS-CoV-2 to humans in Dutch farms were reported by Nature on 1 June 2020 [11].



Rhinolophus sinicus /
Hipposideridae

- SARS-CoV-2 is 96% identical at the whole-genome level to a bat coronavirus.



Canis lupus familiaris

- Confirmed cases in dogs were reported in Hong Kong, New York, Georgia, Texas, South Carolina, etc.

N.A.

Felidae

- Laboratory confirmed cases of cats;

N.A.



- Four tigers and three lions at the same facility were all confirmed with SARS-CoV-2 in New York in April, 2020;
- Confirmed cases in cats in New York, Minnesota, Illinois, California.

Note: N.A. - not available yet.

Hong Kong, Hong Kong Special Administrative Region of the People's Republic of China.

Utah, New York, Georgia, Texas, South Carolina, Minnesota, Illinois, California are states of the United States.

739

740 **Supplementary material**

741 **Supplementary material Supplemental Figure S1-S6, Supplemental Table S1,**
742 **S3 and S6 and Supplemental Methods**

743 **Supplemental Figure S1 ROC curves and AUC values of DeepHoF and BLAST**
744 **on five host types**

745 DeepHoF performs better than BLAST on AUC of each host type.

746 **Supplemental Figure S2 The untenable linear correlations between the lengths**
747 **and the host likelihood scores for genes of SARS-CoV-2**

748 For the genes of SARS-CoV-2, there is no statistical significance in the linear
749 correlations between the lengths and the host likelihood scores on plant (**A**), germ (**B**),
750 invertebrate (**C**), vertebrate (**D**) and human (**E**).

751 **Supplemental Figure S3 Human host likelihood scores of 5 genes of SARS-**
752 **CoV-2, SARS-CoV and MERS-CoV**

753 Although all the three coronaviruses possess ORF1ab and four structural genes (S, M,
754 N, E), these genes made different contributions on human host likelihood scores in
755 these three viruses (two-sided unpaired Welch Two Sample *t*-test, *p*-value < 0.05). S

756 gene and M gene contributed more in SARS-CoV-2 and SARS-CoV, while N gene
757 and E gene were more significant in MERS-CoV.

758 **Supplemental Figure S4 Visualization of the host likelihood score profiles of**
759 **SARS-CoV-2 isolates from different GISAID clades and the manually mutated**
760 **SARS-CoV-2 isolates on two-dimensional PCA**

761 SARS-CoV-2 isolates fall into several clear fusiform clusters with different colors
762 according to their clades. Manually mutated with specific marker variants, the 17
763 earliest sequenced isolates move to the corresponding fusiform cluster of the clade
764 that is represented by the specific marker variants.

765 **Supplemental Figure S5 Six phases of an input sequence**

766 For coding the COH matrix of a given sequence, we represented it with the direct
767 conjunction of its six phases, generated from its complementary strand and itself.

768 **Supplemental Figure S6 Structure of BiPathCNN in DeepHoF**

769 BOH matrix and COH matrix are input into two paths independently and transformed
770 by the convolution and pooling layers at the beginning. A concatenation layer and a
771 normalization layer combine the output of the two paths. Five sub-paths process the
772 combined intermediate output individually. Each sub-path contains a full connection
773 layer, a normalization layer and an output layer with sigmoid activation and binary
774 cross-entropy loss function. The five sub-paths output the host likelihood scores on
775 five host types respectively.

776 **Supplemental Table S1 Comparison of performance of DeepHoF and BLAST on**
777 **each host type classification**

778 **Supplemental Table S3 Top 20 hosts predicted by DeepHoF on SARS-CoV-2**

779 **Supplemental Table S6 Subtypes in five host types**

780 **Other supplementary material for this manuscript includes the following:**

781 **Supplemental Table S2 Metadata and host likelihood scores of genes for SARS-**
782 **CoV, MERS-CoV and SARS-CoV-2 isolates**

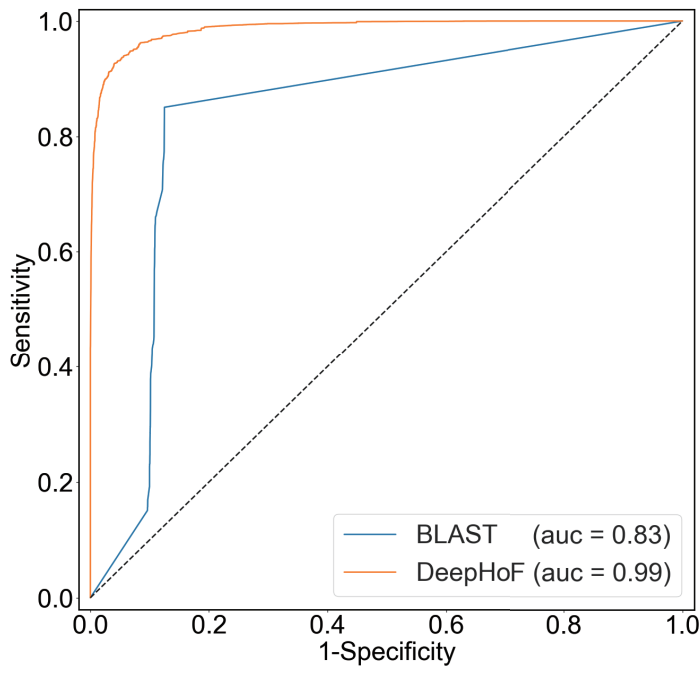
783 **Supplemental Table S4 Contributions of 11 genes in the determination of hosts**
784 **for SARS-CoV-2**

785 **Supplemental Table S5 Metadata, host likelihood score profiles, and high**
786 **frequency SNPs on 53759 SARS-CoV-2 isolates**
787 **Supplemental Table S7 Host information of the viral genomes in training and**
788 **test sets of DeepHoF**
789 **Supplemental Table S8 Acknowledge of sequence data of SARS-CoV-2 in**
790 **GISAID**
791

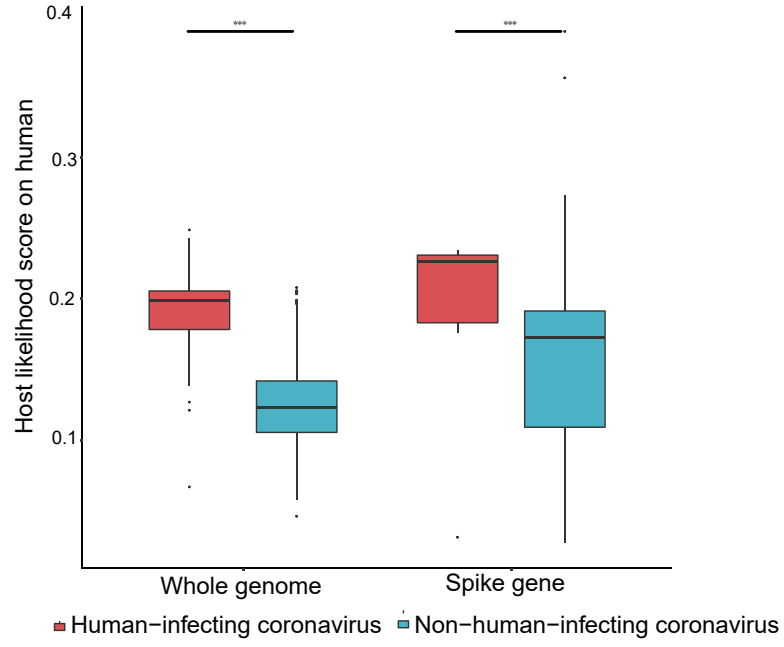
792 **Data statement**

793 Data utilized in the analysis of SARS-CoV-2, including the host likelihood score
794 profiles and the metadata of 53,759 SARS-CoV-2 isolates, are available in the main text
795 and Supplementary Information. The trimmed sequences of 53,759 isolates and the
796 training and test sets of DeepHoF have been deposited on our lab homepage
797 <http://cqb.pku.edu.cn/ZhuLab/DeepHoF/>.
798 The open source code utilized in this study has been deposited on GitHub
799 <https://github.com/PKUBioinfo-ZhuLab/DeepHoF> and our lab homepage
800 <http://cqb.pku.edu.cn/ZhuLab/DeepHoF/>

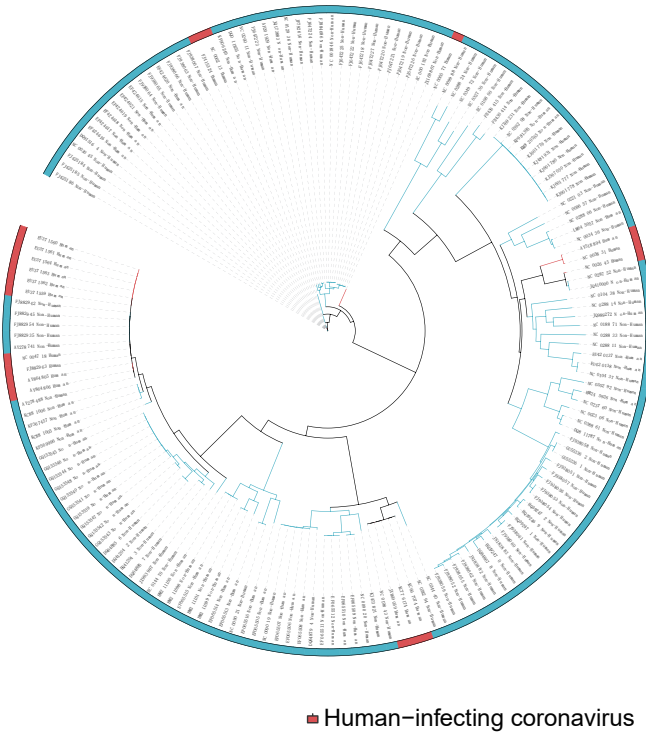
a



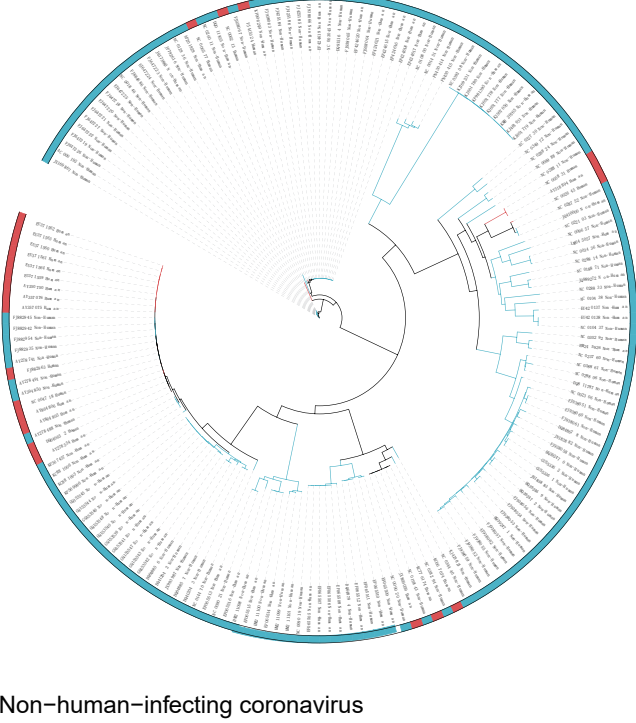
b

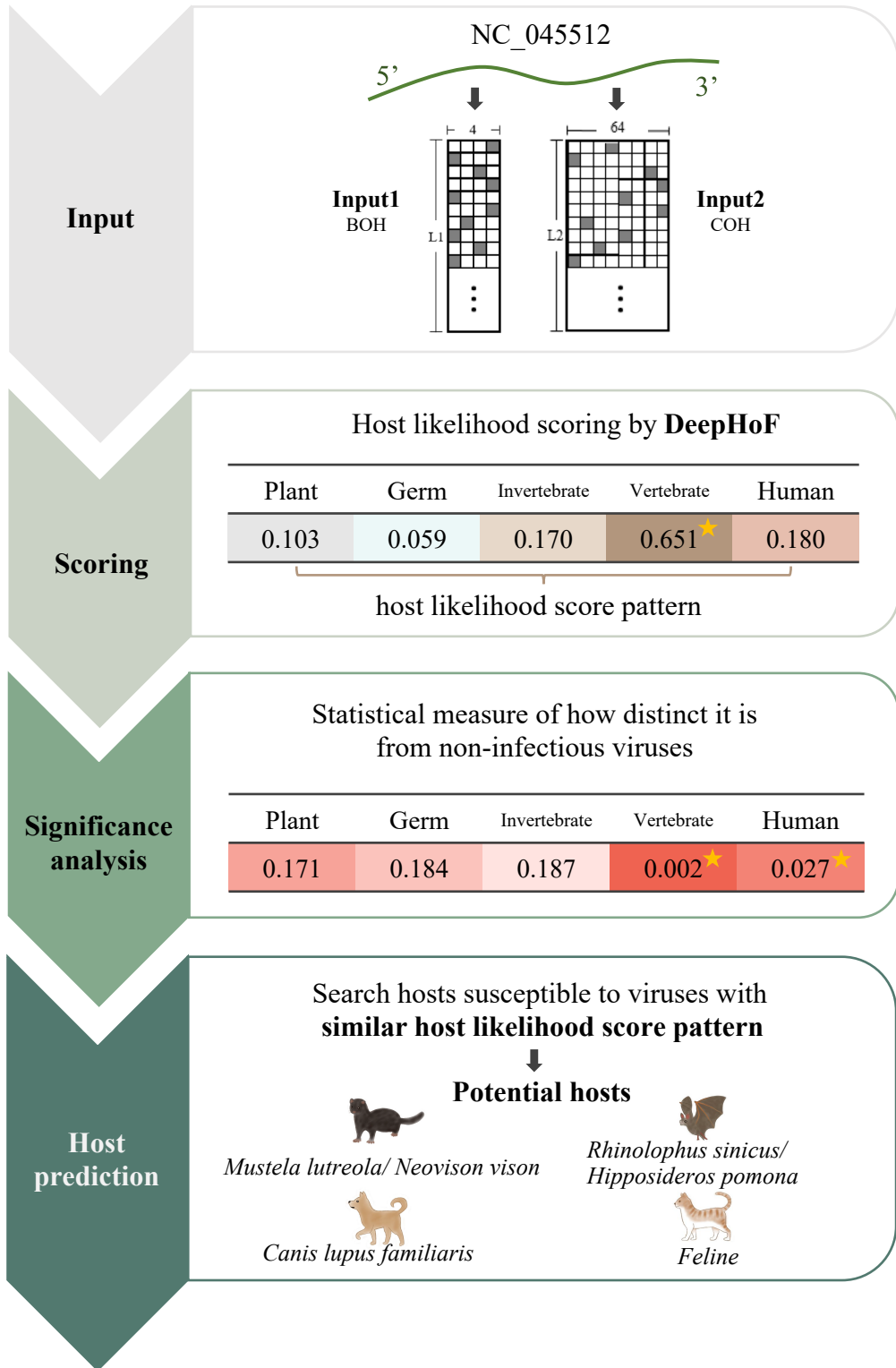


c



d

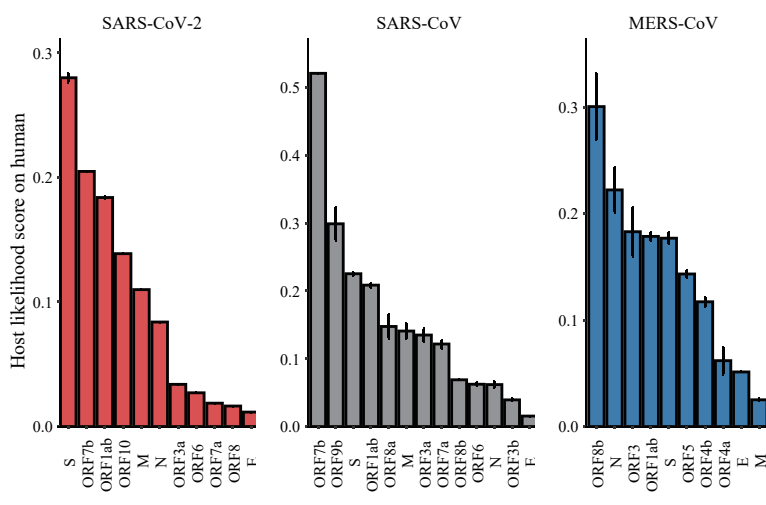




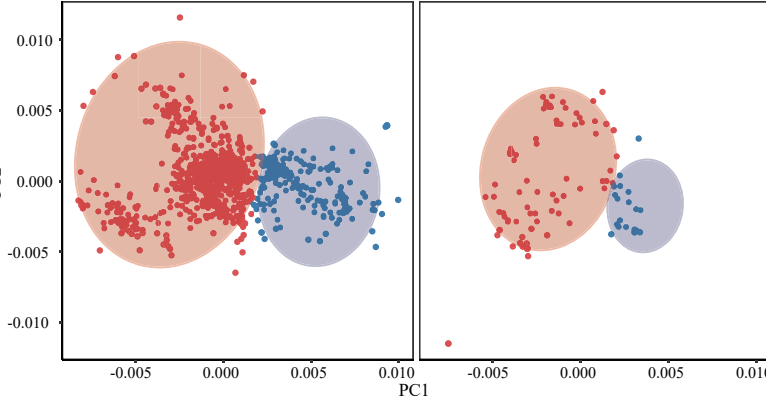
a

Coronavirus	Host likelihood score on human	Significant	Host likelihood score on non-human vertebrate	Significant
Human coronavirus NL63	██████████	Y	██████████	Y
Night-heron coronavirus HKU19	██████████	Y	██████████	Y
Severe acute respiratory syndrome coronavirus	██████████	Y	██████████	Y
Wuhan/HB/DC-HB/01/2019*	██████████	Y	██████████	Y
Wuhan/HB/DC-HB/02/2019*	██████████	Y	██████████	Y
Wuhan/WIV05/2019*	██████████	Y	██████████	Y
Wuhan/HB/DC-HB/02/2019*	██████████	Y	██████████	Y
Wuhan/WIV06/2019*	██████████	Y	██████████	Y
Wuhan/WIV07/2019*	██████████	Y	██████████	Y
Wuhan/WIV02/2019*	██████████	Y	██████████	Y
Wuhan/WH01/2019*	██████████	Y	██████████	Y
Wuhan/IBPCAMS-WH-04/2019*	██████████	Y	██████████	Y
Wuhan/IVDC-HB-01/2019*	██████████	Y	██████████	Y
Wuhan/WIV04/2019*	██████████	Y	██████████	Y
Wuhan/IBPCAMS-WH-02/2019*	██████████	Y	██████████	Y
Wuhan/IVDC-HB-05/2019*	██████████	Y	██████████	Y
Wuhan/IBPCAMS-WH-03/2019*	██████████	Y	██████████	Y
Wuhan/Hu-1/2019*	██████████	Y	██████████	Y
Wuhan/IVDC-HB-GX02/2019*	██████████	Y	██████████	Y
Middle East respiratory syndrome coronavirus				
Wuhan/IBPCAMS-WH-01/2019*	██████████	Y	██████████	Y
Batacoronavirus England 1	██████████	Y	██████████	Y
Bat coronavirus isolate PREdict	██████████	Y	██████████	Y
Thrush coronavirus HKU12-600	██████████	Y	██████████	Y
Camel alphacoronavirus isolate camel	██████████	Y	██████████	Y
White-eye coronavirus HKU16	██████████	Y	██████████	Y
Bulbul coronavirus HKU11-934	██████████	Y	██████████	Y
Bat coronavirus BM48-31/BGR/2008	██████████	Y	██████████	Y
Human coronavirus 229E	██████████	Y	██████████	Y
Common-moorhen coronavirus HKU21	██████████	Y	██████████	Y
Wigeon coronavirus HKU20	██████████	Y	██████████	Y
Batacoronavirus <i>Eriacus</i> VMC	██████████	Y	██████████	Y
Human coronavirus OC43 strain ATCC VR-759	██████████	Y	██████████	Y
Turkey coronavirus	██████████	Y	██████████	Y
Rousettus bat coronavirus HKU10	██████████	Y	██████████	Y
Bovine coronavirus	██████████	Y	██████████	Y
Rabbit coronavirus HKU14	██████████	Y	██████████	Y
Swine enteric coronavirus strain Italy	██████████	Y	██████████	Y
Rat coronavirus Parker, complete genome	██████████	Y	██████████	Y
Bat <i>Hb</i> -betacoronavirus/Zhejiang/2013	██████████	Y	██████████	Y
Munia coronavirus HKU13-3514	██████████	Y	██████████	Y
Bat coronavirus HKU4-1	██████████	Y	██████████	Y
Mink coronavirus strain WDI127	██████████	Y	██████████	Y
Betacoronavirus HKU24 strain HKU24-R050051	██████████	Y	██████████	Y
Ferret coronavirus isolate FRCO-NL-2010	██████████	Y	██████████	Y
Magpie-robin coronavirus HKU18	██████████	Y	██████████	Y
Scotophilus bat coronavirus S12	██████████	Y	██████████	Y
Porcine coronavirus HKU15 strain HKU15-155	██████████	Y	██████████	Y
Bat coronavirus CDPH-E15/USA/2006	██████████	Y	██████████	Y
Bat coronavirus HKU2	██████████	Y	██████████	Y
Rousettus bat coronavirus isolate GCCDC1 356	██████████	Y	██████████	Y
Lucheng Rn rat coronavirus isolate Lucheng-19	██████████	Y	██████████	Y
Sparrow coronavirus HKU17	██████████	Y	██████████	Y
Bat coronavirus 1A	██████████	Y	██████████	Y
Wencheng Sm shrew coronavirus isolate Xingguo-101	██████████	N	██████████	Y
Beluga Whale coronavirus SW1	██████████	N	██████████	Y
NL63-related bat coronavirus strain BtKYNL63-9a	██████████	N	██████████	Y
Bat coronavirus HKU9-1	██████████	N	██████████	Y
Bat coronavirus HKU5-1	██████████	N	██████████	Y
Human coronavirus HKU1	██████████	N	██████████	Y
Bat coronavirus HKU8	██████████	N	██████████	Y

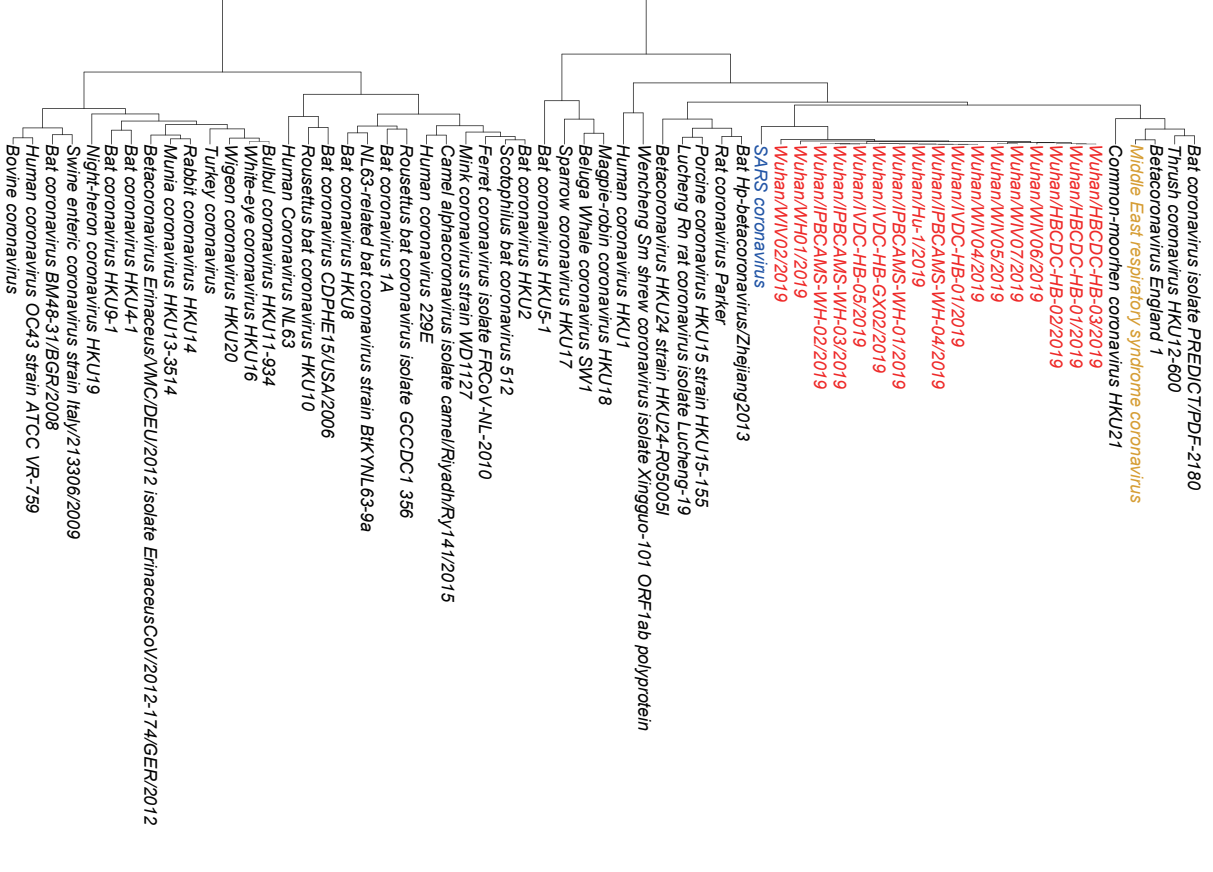
5



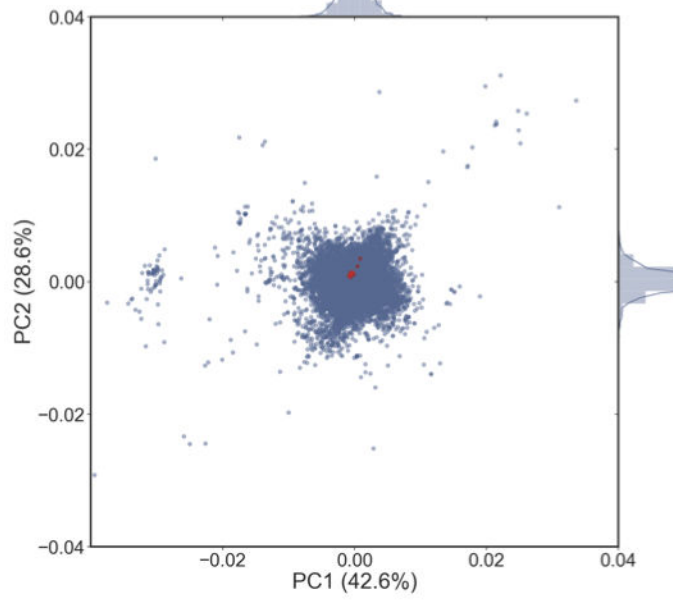
6



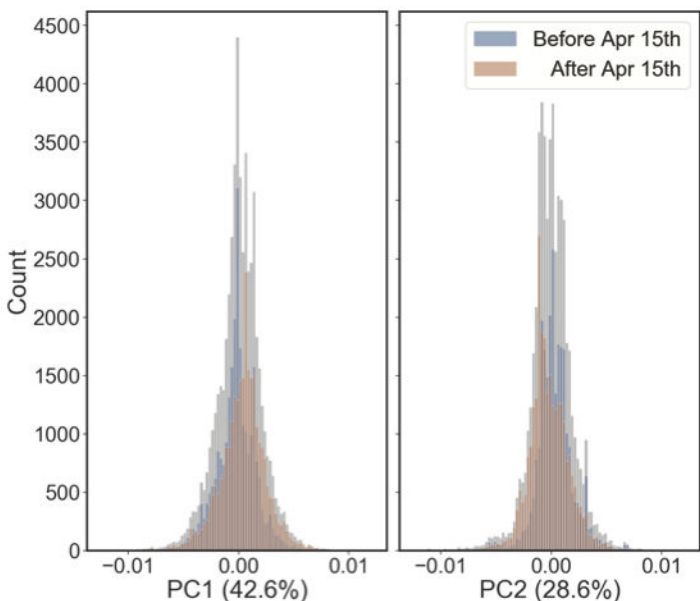
10



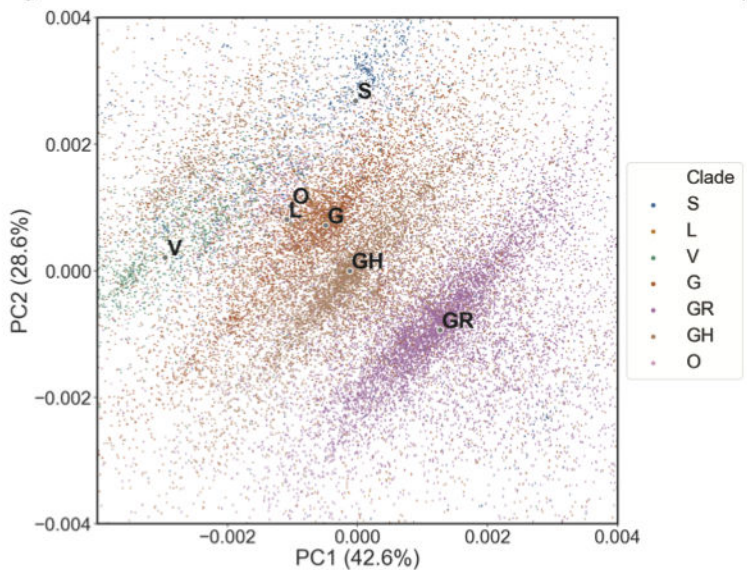
a



b



c



d

